





RESEARCH ARTICLE

Assessing brain involvement in Fabry disease with deep learning and the brain-age paradigm

Alfredo Montella¹ | Mario Tranfa¹  | Alessandra Scaravilli¹ | Frederik Barkhof^{2,3,4,5} | Arturo Brunetti¹ | James Cole^{4,5}  | Michela Gravina⁶ | Stefano Marrone⁶ | Daniele Riccio⁶ | Eleonora Riccio⁷ | Carlo Sansone⁶ | Letizia Spinelli¹ | Maria Petracca^{8,9} | Antonio Pisani⁷ | Sirio Coccozza¹  | Giuseppe Pontillo^{1,2,3,6} 

¹Department of Advanced Biomedical Sciences, University "Federico II", Naples, Italy

²NMR Research Unit, Queen Square MS Centre, Department of Neuroinflammation, UCL Institute of Neurology, London, UK

³Department of Radiology and Nuclear Medicine, MS Center Amsterdam, Amsterdam Neuroscience, Amsterdam UMC, Vrije Universiteit Amsterdam, Amsterdam, The Netherlands

⁴Centre for Medical Image Computing, University College London, London, UK

⁵Dementia Research Centre, UCL Queen Square Institute of Neurology, University College London, London, UK

⁶Department of Electrical Engineering and Information Technology (DIETI), University "Federico II", Naples, Italy

⁷Department of Public Health, Nephrology Unit, University "Federico II", Naples, Italy

⁸Department of Neurosciences and Reproductive and Odontostomatological Sciences, University "Federico II", Naples, Italy

⁹Department of Human Neurosciences, Sapienza University of Rome, Rome, Italy

Correspondence

Sirio Coccozza, Department of Advanced Biomedical Sciences, University "Federico II", Via Pansini 5, 80131 Naples, Italy.
Email: sirio.coccozza@unina.it

Abstract

While neurological manifestations are core features of Fabry disease (FD), quantitative neuroimaging biomarkers allowing to measure brain involvement are lacking. We used deep learning and the brain-age paradigm to assess whether FD patients' brains appear older than normal and to validate brain-predicted age difference (brain-PAD) as a possible disease severity biomarker. MRI scans of FD patients and healthy controls (HCs) from a single Institution were, retrospectively, studied. The Fabry stabilization index (FASTEX) was recorded as a measure of disease severity. Using minimally preprocessed 3D T1-weighted brain scans of healthy subjects from eight publicly available sources ($N = 2160$; mean age = 33 years [range 4–86]), we trained a model predicting chronological age based on a DenseNet architecture and used it to generate brain-age predictions in the internal cohort. Within a linear modeling framework, brain-PAD was tested for age/sex-adjusted associations with diagnostic group (FD vs. HC), FASTEX score, and both global and voxel-level neuroimaging measures. We studied 52 FD patients (40.6 ± 12.6 years; 28F) and 58 HC (38.4 ± 13.4 years; 28F). The brain-age model achieved accurate out-of-sample performance (mean absolute error = 4.01 years, $R^2 = .90$). FD patients had significantly higher brain-PAD than HC (estimated marginal means: 3.1 vs. -0.1 , $p = .01$). Brain-PAD was associated with FASTEX score ($B = 0.10$, $p = .02$), brain parenchymal fraction ($B = -153.50$, $p = .001$), white matter hyperintensities load ($B = 0.85$, $p = .01$), and tissue volume reduction throughout the brain. We demonstrated that FD patients' brains appear older than normal. Brain-PAD correlates with FD-related multi-organ damage and is influenced by both global brain volume and white matter

Alfredo Montella and Mario Tranfa share the first authorship.

Main Institution: University "Federico II," Via Pansini 5, 80131 Naples, Italy.

This is an open access article under the terms of the [Creative Commons Attribution-NonCommercial-NoDerivs](https://creativecommons.org/licenses/by-nc-nd/4.0/) License, which permits use and distribution in any medium, provided the original work is properly cited, the use is non-commercial and no modifications or adaptations are made.

© 2024 The Authors. *Human Brain Mapping* published by Wiley Periodicals LLC.

hyperintensities, offering a comprehensive biomarker of (neurological) disease severity.

KEYWORDS

brain-age, deep learning, Fabry disease, neuroimaging biomarkers, quantitative imaging

Practitioner Points

- Patients with Fabry disease show significantly higher brain-predicted age difference values compared to healthy controls (estimated marginal means: 3.1 vs. -0.1 , $p = .01$).
- Brain-predicted age difference correlates with multi-organ disease severity and is associated with brain parenchymal fraction, white matter hyperintensities load, and tissue volume throughout the brain.
- Brain-predicted age difference might represent a sensitive quantitative biomarker of brain involvement in Fabry disease, with potentially relevant implications for patient stratification and treatment response monitoring.

1 | INTRODUCTION

Fabry disease (FD; OMIM 301500) is a rare X-inherited lysosomal storage disorder characterized by the accumulation of metabolites in various cell types, resulting from the absent or markedly deficient activity of the enzyme α -galactosidase A and leading to damage and loss of function of especially the kidney, heart, and brain (Germain, 2010). The neurological manifestations of FD include both peripheral and central nervous system involvement, with the first manifested by neuropathic pain, reduced cold and warm sensation and gastrointestinal disturbances, and the second being mainly attributable to cerebrovasculopathy, with an increased risk of ischemic stroke (Germain, 2010). From a pathological standpoint, brain involvement is mainly characterized by endothelial lipid deposition and vascular pathology, the severity of which may greatly vary, reflecting the complex pathophysiology of tissue damage in FD (Kolodny et al., 2015). The recommended follow-up of patients with FD includes brain MR imaging, along with cardiac MRI to assess possible left ventricular hypertrophy and myocardial fibrosis (Germain et al., 2022). However, an accurate evaluation of FD-related brain damage is hampered by the lack of quantitative imaging biomarkers (Cocozza, Russo, et al., 2018), which also limits the possibility of monitoring the effectiveness of recently introduced specific treatments on cerebral manifestations (Azevedo et al., 2021). In the search for objective imaging-derived markers of brain health and pathology, a large body of literature has investigated FD-related brain damage using advanced MRI techniques (Cocozza, Russo, et al., 2018), which, however, are not routinely acquired in clinical practice and require long processing time. In this context, the brain-age paradigm has emerged as a promising approach, summarizing neuroimaging data into a simple quantitative biomarker of brain health that can be easily obtained from raw or minimally preprocessed T1w scans which are often available in routine MRI examinations, making it particularly suitable for immediate clinical application in real-world scenarios (Cole & Franke, 2017). Briefly, machine-learning methods are used to model

chronological age as a function of structural brain MRI scans in healthy people, and the resulting model of “normal” brain aging is used for neuroimaging-based age prediction in unseen subjects (Cole & Franke, 2017). The extent to which each subject deviates from healthy brain-aging trajectories, expressed as the difference between predicted and chronological age (the brain-predicted age difference, brain-PAD), has been proposed as an index of structural brain health, sensitive to pathology in a wide spectrum of neurological and psychiatric disorders (Kaufmann et al., 2019). As a relevant example, brain-age predictions are sensitive to white matter hyperintensities (WMH) and brain volumes, imaging features that are both manifestations of cerebral small vessel disease (Lee et al., 2022; Shi et al., 2022; Wagen et al., 2022), which is thought to be the main pathogenetic mechanisms through which FD impacts brain health (Kolodny et al., 2015).

Here, we applied the brain-age paradigm to investigate brain involvement in patients with FD. Our main aims were: (i) to assess whether FD brains deviate from normal aging trajectories; (ii) to validate brain-PAD as a measure of disease severity against other established clinical markers; and (iii) to explore the neuroimaging determinants of brain-age prediction in this condition.

2 | MATERIALS AND METHODS

2.1 | Participants

In this retrospective, cross-sectional study, part of a larger monocentric research program on FD (Cocozza et al., 2018; Cocozza et al., 2020; Gabusi et al., 2022; Pontillo et al., 2018) patients with a genetically confirmed diagnosis were selected (Vardarli et al., 2020), along with age- and sex-comparable healthy controls (HCs). Participants with history of major cerebrovascular events were excluded. Additional exclusion criteria were age <18 or >65 years, and the presence of other relevant neurological or systemic conditions, leading to

a final number of 52 patients with FD (40.6 ± 12.6 years; M/F: 24/28) and 58 HC (38.4 ± 13.4 years; M/F: 30/28).

Scores quantifying the involvement of nervous, renal and cardiac systems in FD patients were computed based on clinical variables recorded within 1 month from the MRI and summed to obtain a cumulative measure of multi-organ damage severity, the total raw Fabry stabilization index (FASTEX) score, ranging from 0 (normal) to 28 (maximum severity) (Mignani et al., 2016).

The study was conducted in compliance with ethical standards and approved by the local ethics committee “Carlo Romano.” Written informed consent was obtained from all participants according to the Declaration of Helsinki.

2.2 | MRI acquisition and preprocessing

All MRI examinations were acquired between October 2015 and April 2019 using the same 3T scanner (Magnetom Trio, Siemens Healthineers), equipped with an eight-channel head coil. The acquisition protocol included a 3D T1-weighted magnetization prepared rapid acquisition gradient echo sequence (TR = 1900 ms; TE = 3.4 ms; TI = 900 ms; flip angle = 9° ; voxel size = $1 \times 1 \times 1$ mm³; 160 axial slices) and, for FD patients, a 3D T2-weighted fluid attenuated inversion recovery (FLAIR) sequence for WMH assessment (TR = 6000 ms; TE = 396 ms; TI = 2200 ms; flip angle = 120° ; voxel size = $1 \times 1 \times 1$ mm³; 160 sagittal slices).

For FD patients, WMH were automatically segmented on FLAIR images using Lesion Segmentation Tool v3.0.0 (www.statistical-modelling.de/ist.html); individual lesion probability maps were then binarized (thresholding at 0.5 probability) to compute WMH burden and to fill lesions in T1-weighted images for subsequent processing steps via LST's default lesion filling procedure. We did not segment WMH in the HC group as a 3D FLAIR sequence was not available for all subjects and the prevalence and load of WMH, as visually assessed on 2D T2-weighted sequences, was negligible.

For all participants, we used the Computational Anatomy Toolbox v12.8 (<http://www.neuro.uni-jena.de/cat>) to segment lesion-filled T1w volumes into gray matter (GM), white matter (WM), and cerebrospinal fluid and obtain MNI-normalized, modulated, smoothed (1 mm full-width at half-maximum isotropic Gaussian kernel) GM and WM probability maps. Summary measures of GM, WM, cerebrospinal fluid, and total intracranial (TIV) volumes were also generated, and brain parenchymal fraction (BPF) was computed as the ratio of brain volume to TIV.

2.3 | Brain-age modeling

A conceptual outline of the different steps of the brain-age modeling procedure is displayed in Figure 1.

Briefly, a model of healthy brain aging was trained and evaluated on a large external dataset (total $N = 2160$; male/female = 1293/867; mean age = 33 years, age range = 4–86) comprising 3D T1-weighted brain scans of healthy subjects from eight publicly available sources (Supplementary Table 1).

Raw T1w volumes underwent minimal preprocessing, including DICOM to Nifti conversion, correction for intensity nonuniformity with N4 bias field correction (Tustison et al., 2010), rigid registration to the MNI space and resampling to 1.5 mm³ voxels, to reduce array size and ensure consistency of spatial orientation and resolution. Finally, images were intensity-normalized by subtracting the image mean and dividing by the image standard deviation.

Our brain-age model was based on a three-dimensional DenseNet architecture (Huang et al., 2017), which has been previously used successfully for brain-age prediction tasks (Wood et al., 2022) and is available as a pre-built network in the Project MONAI library (https://docs.monai.io/en/stable/_modules/monai/networks/nets/densenet.html). We used the DenseNet264 version and adapted it by adding a linear regression layer for the prediction of a continuous variable and a 0.2 dropout rate after each dense layer to reduce the risk of overfitting. Modeling was performed with PyTorch 1.12.0 (Paszke

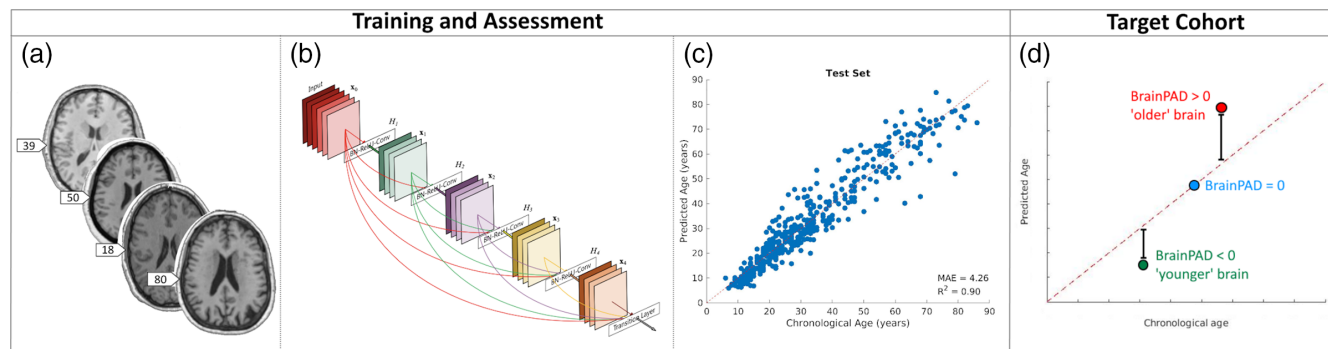


FIGURE 1 Outline of the brain-age modeling procedure. Minimally preprocessed T1-weighted images (a) are used as input for the training and the evaluation of a model for the prediction of chronological age based on a 3D DenseNet architecture (b). The model with the lowest validation loss is chosen, and performance is measured on the previously unseen cases of the test set (c). The final model is also applied to the target clinical population (d), composed of the internal cohort of FD patients and HC, to generate brain-predicted ages and corresponding brain-PAD values. Brain-PAD, brain-predicted age difference; FD, Fabry disease; HC, healthy controls; MAE, mean absolute error.

et al., 2019) using one NVIDIA Tesla V100S 32 GB graphics processing unit. The full dataset was randomly split into training (64% = 1382), validation (16% = 346), and test (20% = 432) sets (Supplementary Figure 1). Mean absolute error and coefficient of determination (R^2) were used to quantify model performance. Age-related bias (i.e., the underestimation of age in older subjects and vice versa) was statistically corrected for using a linear model estimated in the training set, as suggested in de Lange et al. (2019).

The final model was applied to minimally preprocessed T1w volumes of the internal cohort of FD patients and HC to generate brain-predicted ages and corresponding brain-PAD values. To scrutinize model predictions in the internal cohort, we used guided backpropagation (Springenberg et al., 2015) to obtain saliency maps highlighting regions of the input image that are most influential for the model's predictions.

To confirm that our results were not driven by contingent methodological choices in terms of model architecture/preprocessing steps, we conducted a sensitivity analysis using age predictions (and brain-PAD values) on the internal cohort obtained using the DeepBrainNet algorithm, a model based on a two-dimensional Inception-ResNet-v2 architecture that takes minimally preprocessed (N4 bias field corrected, skull-stripped, and affinely registered to the MNI space) T1w images as input and has been extensively validated (Bashyam et al., 2020).

2.4 | Statistical analysis

Unless otherwise specified, statistical analyses were carried out using the Statistical Package for Social Science (SPSSv25.0, IBM corp.), with a statistical significance level $\alpha = .05$ and 95% confidence intervals (CI) and p values computed using bootstrap with 1000 resamples.

To assess possible between-group differences in terms of brain-PAD, we used one-way ANCOVA, controlling for the effects of age, age² (to account for the nonlinear effect of age), and sex, and calculating estimated marginal means for the two groups.

To validate brain-PAD as a measure of disease severity, we tested its association with the FASTEX score in a linear regression model including also age, age², and sex. Similar models were used to test the association between the FASTEX score and conventional MRI measures (BPF and WMH burden).

To investigate the neuroimaging determinants of brain-PAD in patients with FD, we used hierarchical linear regression analyses with age, age², and sex in the first block and WMH load or BPF in the second block. Similarly, we tested age-, age²-, and sex-adjusted associations between brain-PAD and TIV-scaled, preprocessed GM, and WM maps, using a nonparametric approach based on 5000 permutations applied to the general linear model (Winkler et al., 2014) via the Threshold Free Cluster Enhancement toolbox (<http://www.neuro.uni-jena.de/tfce>). The same analysis was repeated after adding the variables group and group \times brain-PAD interaction in the model, with this latter term intended to test the hypothesis that different voxel-wise patterns might influence brain-age prediction in the two groups.

3 | RESULTS

A flow diagram summarizing the patient selection procedure is shown in Figure 2. A total of 52 patients with FD were identified (40.6 ± 12.6 years; M/F: 24/28), along with 58 HC (38.4 ± 13.4 years; M/F: 30/28). The median FASTEX score of FD patients was 6 (interquartile range 3–9), indicating mild-to-moderate involvement. Complete demographic, clinical, and MRI characteristics of the studied population are available in Table 1.

The brain-age model trained on healthy subjects' MRI scans achieved an accurate out-of-sample age prediction (test set mean absolute error = 4.01 years, $R^2 = .90$). The interpretability analysis on the internal cohort showed that the model focused on regions that appear to be primarily related to (the widening of) the cerebrospinal fluid spaces (Figure 3).

When looking at brain-PAD values in the two groups, there was a significant difference while correcting for age, age², and sex ($F[1, 105] = 6.46$, $p = .01$, partial $\eta^2 = 0.06$), with FD patients showing higher values than HC (estimated marginal means 3.1 [95% CI = 1.0–5.3] vs. -0.1 [95% CI = -1.9 to 1.4]) (Figure 4). Similar results were obtained when considering DeepBrainNet-derived brain-age predictions ($F[1, 105] = 5.02$, $p = .03$, partial $\eta^2 = 0.05$; estimated marginal means: FD, 4.1 [95% CI = 2.3–6.0] vs. HC, 1.2 [95% CI = -0.5 to 3.0]) (Supplementary Figure 2). When assessing the agreement between the two models at the subject-level, there was a strong correlation between brain-predicted ages ($r = .84$, $p < .001$) (Supplementary Figure 3).

Brain-PAD was significantly associated with the FASTEX score ($B = 0.10$ [95% CI = 0.02–0.19]; standard error $B = 0.04$; $p = .02$), in a linear model including also age, age², and sex ($R^2 = .41$, $p < .001$),

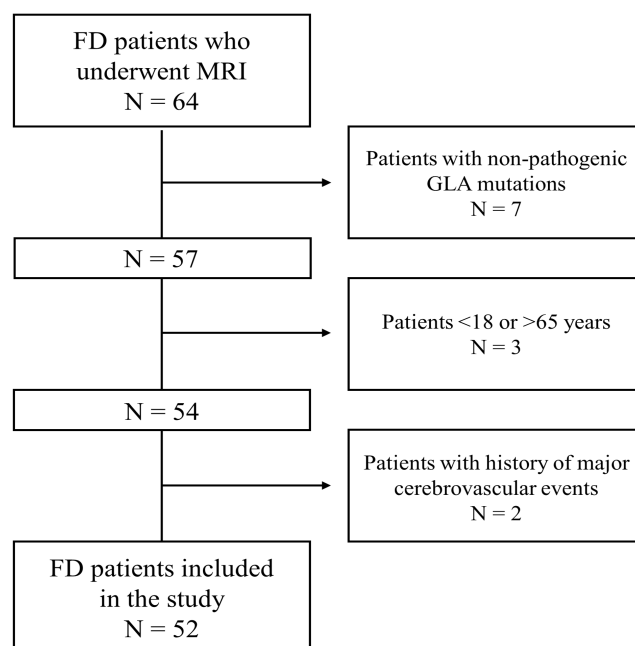


FIGURE 2 Flow diagram summarizing the patient selection procedure. FD, Fabry disease; GLA, α -galactosidase A.

TABLE 1 Demographic, clinical, and MRI characteristics of all the participants included in the study.

	FD N = 52	HC N = 58	p-Value (FD vs. HC)
Age (years)	40.6 ± 12.6	38.4 ± 13.4	.37
Sex (M/F) ^a	24/28	30/28	.56
Treatment (Y/N) ^a	29/23	n.a.	n.a.
Treatment duration (years) ^b	1.8 (1.2–2.3)	n.a.	n.a.
FASTEX score ^b			
Total score	6 (3–9)	n.a.	n.a.
Nervous system score	2 (1–2)	n.a.	n.a.
Renal system score	1 (1–3)	n.a.	n.a.
Cardiac system score	2 (1–3)	n.a.	n.a.
BPF	0.81 ± 0.03	0.82 ± 0.03	.06
WMH load (ml) ^b	0.3 (0.0–0.6)	n.a.	n.a.
Brain-PAD (years) ^c	3.1 (0.9)	–0.1 (0.9)	.01

Note: Unless otherwise specified, data are expressed as mean ± standard deviation. Between-group differences were tested with either Student *t* (age and BPF) or chi-square (sex) tests.

Abbreviations: BPF, brain parenchymal fraction; FD, Fabry disease; HC, healthy control; n.a., not applicable; SD, standard deviation; WMH, white matter hyperintensities.

^aExpressed as number of subjects.

^bExpressed as median, with interquartile range in parentheses.

^cExpressed as age, age², and sex-adjusted estimated marginal mean, with standard error in parentheses.

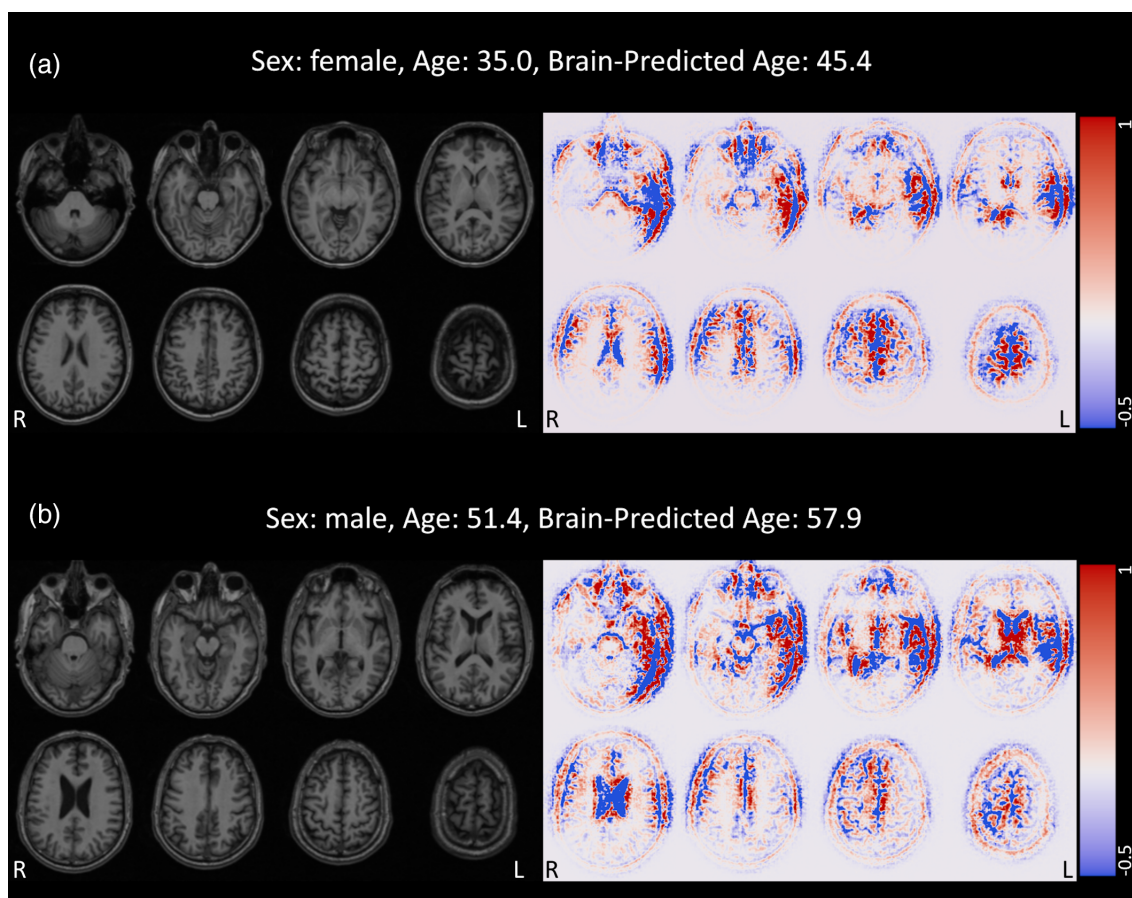


FIGURE 3 Saliency maps of two representative patients with FD. Light box view of selected slices from the minimally preprocessed T1w volumes (on the left) and corresponding guided backpropagation-derived maps (on the right) of one female (a) and one male (b) patients with FD. For saliency maps, both positive (positively correlated with the output, in red) and negative (negatively correlated with the outcome, in blue) magnitudes are shown. In both cases, the model focuses mostly on regions that appear to be related to (the widening of) the cerebrospinal fluid spaces. FD, Fabry disease.

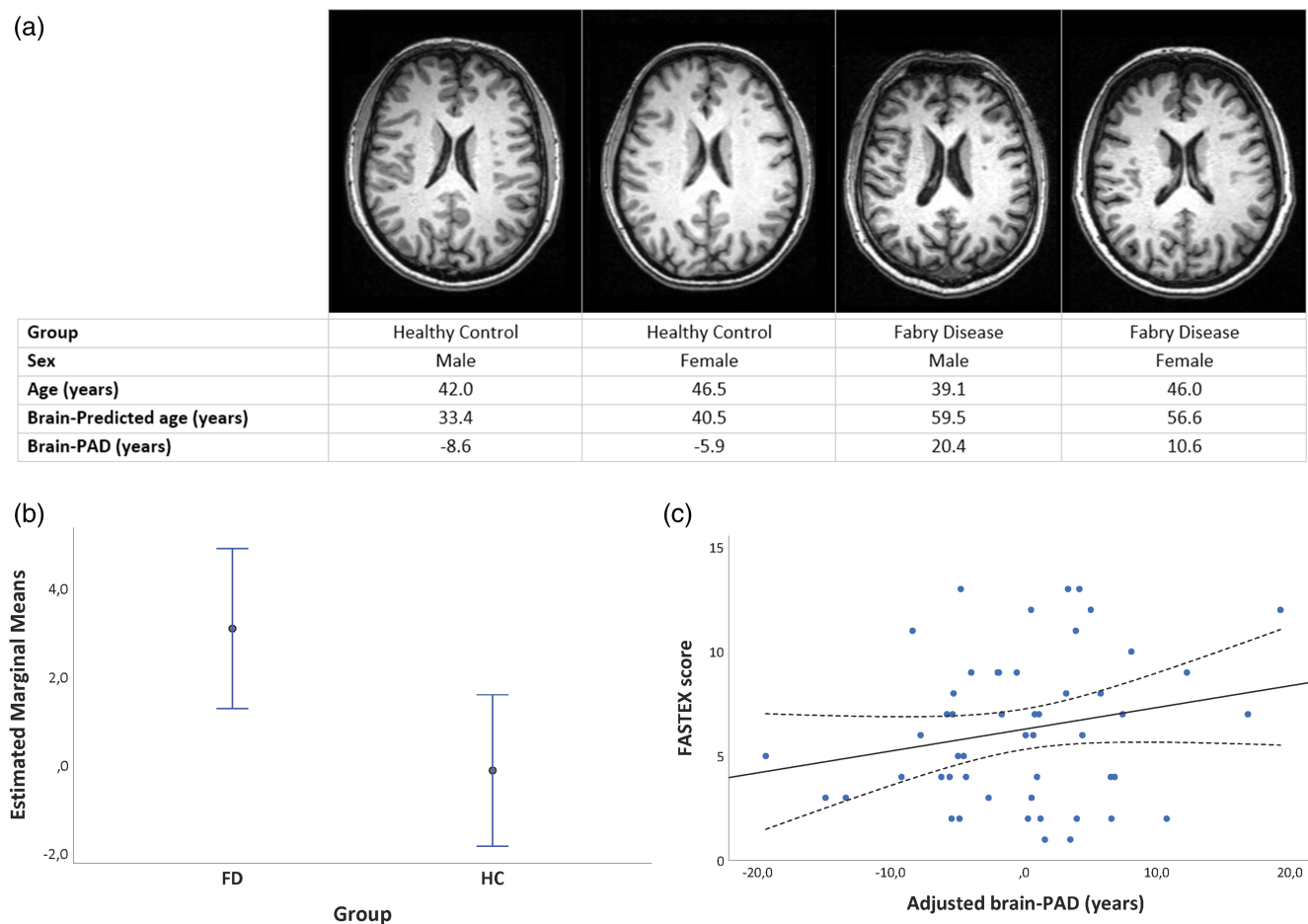


FIGURE 4 Brain-age prediction in the internal cohort and its relationship with disease status (FD vs. HC) and the FASTEX score. In (a), presented are comparable-level axial slices from four example subjects (two per group) with extreme brain-PAD values. In (b), age, age², and sex-adjusted estimated marginal means for the two groups, along with 95% bootstrap confidence intervals. In (c), scatterplot showing the relationship between brain-PAD values (age, age², and sex-adjusted) and FASTEX score in patients with FD. brain-PAD, brain-predicted age difference; FASTEX, Fabry stabilization index; FD, Fabry disease; HC, healthy controls.

corresponding to a 0.10 increase in the FASTEX score for each additional year of brain-predicted age (Figure 4). As for conventional MRI measures, no significant associations emerged between the FASTEX score and either BPF ($B = 10.65$ [95% CI = -21.00 to 36.33]; standard error $B = 14.66$; $p = .49$) or WMH burden ($B = 0.16$ [95% CI = -0.17 to 5.26]; standard error $B = 0.84$; $p = .21$).

As for the neuroimaging determinants of brain-PAD in FD patients, both higher WMH load ($p = .01$) and lower BPF ($p = .001$) were associated with older-appearing brains (Table 2). Voxel-wise, we found a significant inverse correlation between brain-PAD values and tissue volumes diffusely throughout the brain, with the strongest effect sizes observed at the level of the deep and periventricular WM (Figure 5). The interaction analysis revealed no significant effect of diagnostic group on the relationship between local tissue volumes and brain-PAD.

4 | DISCUSSION

By applying the brain-age paradigm in a relatively large cohort of patients, we found that FD is associated with older-appearing brains

(on average, 3 years more than normal), indicative of accelerated cerebral aging. The brain-PAD metric correlates with FD-related multi-organ damage and is influenced by both global brain volume and WMH load.

We used deep learning for age-prediction as it outperforms more traditional machine learning methods when using large and diverse MRI datasets and can generate accurate predictions on raw or quasi-raw MRI data, thus having greater potential for real-time application in clinical settings (Tanveer et al., 2023). Our brain-age model was built using an “off-the-shelf” DenseNet264 configuration, to ensure reproducibility and ease of use. Interestingly, not only the achieved performance was close to that of literature benchmarks (Leonardsen et al., 2022; Wood et al., 2022), but the model of healthy brain aging was also sensitive to FD-related cerebral pathology. Also relevant for clinical translatability, the interpretability analysis showed that model predictions in FD patients appear to be guided by biologically meaningful features, which are mostly related to cortical and subcortical atrophy, potentially capturing subject-specific neuroanatomic patterns. Of note, the sensitivity of the brain-age paradigm to FD was also confirmed when using the DeepBrainNet model, suggesting that

our findings are relatively robust to methodological choices in terms of preprocessing steps and neural network architecture.

Brain involvement in FD is thought to be mainly mediated by lysosomal deposition of catabolites in endothelial cells, leading to micro- and macro-vascular manifestations that partly overlap with those occurring in common small vessel disease and normal aging (Rost et al., 2016). Uncertainty exists on the relative importance of a

TABLE 2 Results of the hierarchical linear regression analyses for the prediction of brain-PAD in FD patients. Confidence intervals, standard errors, and *p* values are based on 1000 bootstrap samples.

	B (95% CI)	SE B	<i>p</i>
<i>Model 1</i>			
Constant	10.48 (−6.00–35.60)	9.41	.23
Age	−0.12 (−1.19–0.71)	0.54	.82
Age ²	−0.002 (−0.016–0.017)	0.007	.75
Sex	1.65 (−2.48–6.14)	2.13	.45
<i>Model 2</i>			
Constant	8.53 (−7.32–39.21)	8.85	.29
Age	0.04 (−0.94–0.73)	0.50	.93
Age ²	−0.005 (−0.017–0.012)	0.006	.43
Sex	0.53 (−3.37–4.13)	2.04	.80
WMH load	0.85 (−2.35–6.78)	1.72	.01
<i>Model 3</i>			
Constant	148.47 (77.24–224.90)	36.81	.001
Age	−0.54 (−1.76–0.27)	0.54	.30
Age ²	0.000 (−0.012–0.017)	0.007	.96
Sex	0.71 (−3.21–4.86)	1.91	.73
BPF	−153.50 (−236.42 to −73.24)	38.74	.001

Note: R^2 is .18 for Model 1, 0.32 ($\Delta R^2 = .14$) for Model 2, and 0.43 ($\Delta R^2 = .25$) for Model 3.

Abbreviations: BPF, brain parenchymal fraction; CI, confidence interval; SE, standard error; WMH, white matter hyperintensities.

possible direct brain tissue damage through lysosomal deposition at the level of other cell types (i.e., neuronal or glial cells) (Schiffmann & Moore, 2006). Interestingly, the accumulation of lysosomal storage bodies in microglia subsets is a physiological process that increases linearly with aging, suggesting a convergence of mechanisms operating during normal aging and in lysosomal storage disorders, with the accumulation of storage bodies potentially driving microglia dysfunction and contributing to neurodegeneration (Burns et al., 2020). Taken together, these observations reinforce the analogy between FD and accelerated aging, with brain-PAD as a plausible neuroimaging biomarker of progressive FD-related brain damage. On the other hand, FD has been also described as a neurodevelopmental disorder (Pontillo et al., 2018), and brain-age predictions are known to be influenced by early-life factors related to brain development (Vidal-Pineiro et al., 2021). Therefore, we cannot exclude that abnormal neurodevelopment might play a role in the observed group differences in terms of brain-predicted age.

The clinical relevance of brain-PAD in FD is illustrated by a significant association with overall, multi-organ, clinical severity in patients. An intricate network of mutual interdependencies exists between brain-age and other bodily (patho)physiological aging phenomena (Cole et al., 2019; Tian et al., 2022). Brain health is shaped by other systems in the body, with cardiovascular and renal (mal)functioning known to have a potentially major impact (Cherbuin et al., 2021; Steinbach & Harshman, 2022; Wagen et al., 2022). Likewise, common, genetically determined, mechanisms may underlie the development of FD-related damage in different organs in parallel.

From a neuroimaging perspective, brain-age predictions in patients with FD were influenced by WMH and brain volume, with no anatomical specificity other than greater effect sizes observed at the level of the deep and periventricular WM, which are known to be preferentially impacted by FD-related lesions and microstructural damage (Ulivi et al., 2020). Our results are in line with previous evidence, confirming the role of a smaller brain volume, rather than the

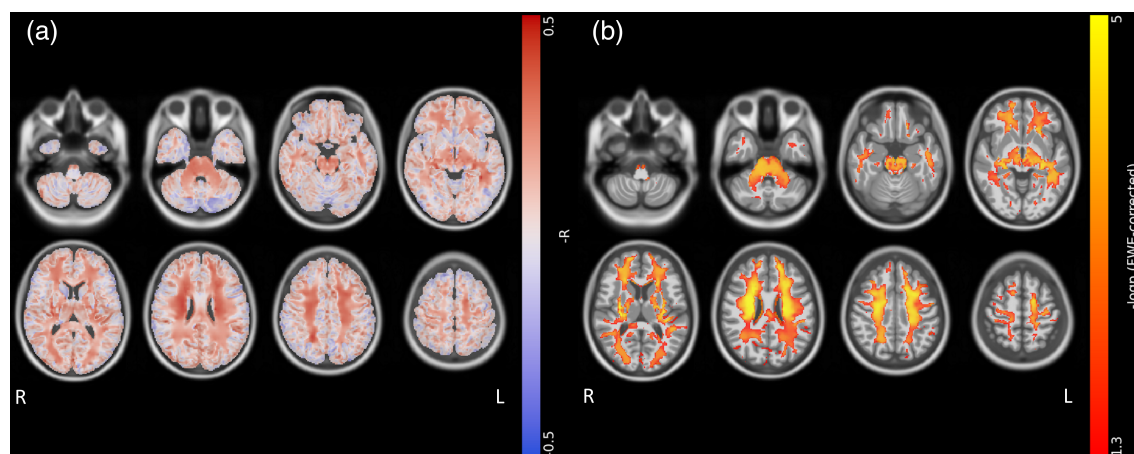


FIGURE 5 Voxel-wise correlation between brain tissue volumes and brain-PAD in patients with FD. (a) Effect size (−R, red to blue) and (b) thresholded statistical (−log_p, yellow to red) maps are shown, superimposed on axial sections of a 3D T1-weighted template in standard space. Brain-PAD, brain-predicted age difference; FD, Fabry disease.

atrophy of specific regions, and a greater WMH burden as the main neuroimaging correlates of higher brain-PAD values (Leonardsen et al., 2022; Wagen et al., 2022; Wood et al., 2022), with no FD-specific determinants emerging from the interaction analysis. Nevertheless, it should be noted that, while the results of the interpretability analysis, the voxel-wise correlations, and the sensitivity analysis on skull-stripped images all show that age predictions are driven by brain features, a minor contribution of non-brain tissues of the skull/scalp cannot be fully excluded (Cali et al., 2023).

Interestingly, several structural MRI studies using more traditional approaches (i.e., voxel-based morphometry and region of interest-based analyses) have failed to reveal consistent changes of brain morphometry in FD patients compared to HC (Cocozza et al., 2018; Cocozza, Russo, et al., 2018; Paavilainen et al., 2013), at least partially because of the small sample sizes. In this light, brain-PAD might represent a more comprehensive biomarker of brain structural health in FD, potentially more sensitive than conventional methods.

Overall, our findings support the role of brain-PAD as a sensitive quantitative biomarker of FD severity, with potentially relevant implications for patient stratification in clinical and research settings, especially in relation to the assessment of treatment response. Indeed, the efficacy of recently introduced specific treatments for FD on cerebral involvement has remained unclear so far, partly because of the very lack of objective neuroimaging measures of disease severity (Feldt-Rasmussen et al., 2020; Rombach et al., 2014).

The main limitation of our study lies in its cross-sectional nature. As mentioned, disentangling the relative effects of neurodevelopmental factors and ongoing pathological processes on brain-PAD is challenging in a cross-sectional setting (Di Biase et al., 2023). Assuming that the impact of neurodevelopment remains constant over time, longitudinal studies are warranted, where brain-predicted age deltas ideally depend solely on ongoing healthy/pathological aging phenomena. Also, a longitudinal design would allow to assess the prognostic value of brain-PAD toward clinical outcomes and evaluate the possible effect of treatment. Furthermore, it is worth noting that, while being sensitive to FD, the brain-PAD metric could be influenced by common comorbidities and therefore may not represent a specific disease biomarker (Cherbuin et al., 2021; Steinbach & Harshman, 2022; Wagen et al., 2022). In this light, crossing brain MRI-derived metrics with additional, more specific, biomarkers of disease severity (e.g., plasma Lyso-Gb3 levels) (Nowak et al., 2022) would help to link brain-PAD more closely to FD pathogenesis. In addition, while the size of our cohort is in line with those of previous studies (Cocozza et al., 2018; Cocozza, Russo, et al., 2018; Paavilainen et al., 2013), replication in larger datasets would help corroborate our findings. Also, brain-age models relying on modalities that are more sensitive to WMH (e.g., FLAIR or diffusion-weighted scans) might be more informative and add to T1w-based models for explaining FD-related brain damage. Finally, as the disease severity in our cohort ranged from mild to moderate, further studies will be needed to test the brain-age paradigm in patients with severe FD.

In conclusion, we provide evidence that the brains of patients with FD appear older than normal. The brain-PAD metric is sensitive

to FD-related brain damage and is associated with systemic involvement, positioning it as a relevant quantitative imaging biomarker to assess (neurological) disease severity in clinical and research settings.

ACKNOWLEDGMENTS

We thank the study participants.

FUNDING INFORMATION

This research received no specific grant from any funding agency in the public, commercial, or not-for-profit sectors.

CONFLICT OF INTEREST STATEMENT

F.B.: Steering committee and iDMC member for Biogen, Merck, Roche, Eisai. Consultant for Roche, Biogen, Merck, IXICO, Jansen, Combinostics. Research agreements with Novartis, Merck, Biogen, GE, Roche. Co-founder and shareholder of Queen Square Analytics LTD. M.P. discloses travel/meeting expenses from Novartis, Janssen, Roche and Merck, speaking honoraria from HEALTH&LIFE S.r.l. and AIM Education S.r.l., honoraria for consulting services from Biogen and research grants from Baroni Foundation. S.C. serves on scientific advisory board for Amicus Therapeutics, has received speaker honoraria from Sanofi and research grants from Fondazione Italiana Sclerosi Multipla and Telethon. G.P. was supported by the MAGNIMS/ECTRIMS (2020) and ESNR (2021) research fellowship programs. The remaining authors of this manuscript declare no relationships with any companies, whose products or services may be related to the subject matter of the article.

DATA AVAILABILITY STATEMENT

The trained brain-age model will be made available at <https://github.com/NeuroN-Lab>. The data that support the findings of this study are available on request from the authors.

ORCID

Mario Tranfa  <https://orcid.org/0000-0002-4451-4746>

James Cole  <https://orcid.org/0000-0003-1908-5588>

Sirio Cocozza  <https://orcid.org/0000-0002-0300-5160>

Giuseppe Pontillo  <https://orcid.org/0000-0001-5425-1890>

REFERENCES

- Azevedo, O., Cordeiro, F., Gago, M. F., Miltenberger-Miltenyi, G., Ferreira, C., Sousa, N., & Cunha, D. (2021). Fabry disease and the heart: A comprehensive review. *International Journal of Molecular Sciences*, 22, 4434.
- Bashyam, V. M., Erus, G., Doshi, J., Habes, M., Nasrallah, I. M., Truelove-Hill, M., Srinivasan, D., Mamourian, L., Pomponio, R., Fan, Y., Launer, L. J., Masters, C. L., Maruff, P., Zhuo, C., Völzke, H., Johnson, S. C., Fripp, J., Koutsouleris, N., Satterthwaite, T. D., ... Davatzikos, C. (2020). MRI signatures of brain age and disease over the lifespan based on a deep brain network and 14468 individuals worldwide. *Brain*, 143, 2312–2324.
- Burns, J. C., Coteleur, B., Walther, D. M., Bajrami, B., Rubino, S. J., Wei, R., Franchimont, N., Cotman, S. L., Ransohoff, R. M., & Mingueneau, M. (2020). Differential accumulation of storage bodies with aging defines discrete subsets of microglia in the healthy brain. *Elife*, 9, e57495.

- Cali, R. J., Bhatt, R. R., Thomopoulos, S. I., Gadewar, S., Gari, I. B., Chattopadhyay, T., Jahanshad, N., & Thompson, P. M. (2023). The influence of brain MRI defacing algorithms on brain-age predictions via 3D convolutional neural networks. *bioRxiv*:2023.04.28.538724.
- Cherbuin, N., Walsh, E. I., Shaw, M., Lunders, E., Anstey, K. J., Sachdev, P. S., Abhayaratna, W. P., & Gaser, C. (2021). Optimal blood pressure keeps our brains younger. *Frontiers in Aging Neuroscience*, 13, 694982.
- Cocozza, S., Pontillo, G., Quarantelli, M., Saccà, F., Riccio, E., Costabile, T., Olivo, G., Brescia Morra, V., Pisani, A., Brunetti, A., Tedeschi, E., & AFFINITY study group. (2018). Default mode network modifications in Fabry disease: A resting-state fMRI study with structural correlations. *Hum Brain Mapping*, 39, 1755–1764.
- Cocozza, S., Russo, C., Pontillo, G., Pisani, A., & Brunetti, A. (2018). Neuroimaging in Fabry disease: Current knowledge and future directions. *Insights Imaging*, 9, 1077–1088.
- Cocozza, S., Schiavi, S., Pontillo, G., Battocchio, M., Riccio, E., Caccavallo, S., Russo, C., Di Risi, T., Pisani, A., Daducci, A., & Brunetti, A. (2020). Microstructural damage of the cortico-striatal and thalamo-cortical fibers in Fabry disease: A diffusion MRI tractometry study. *Neuroradiology*, 62, 1459–1466.
- Cole, J. H., & Franke, K. (2017). Predicting age using neuroimaging: Innovative brain ageing biomarkers. *Trends in Neuroscience*, 40, 681–690.
- Cole, J. H., Marioni, R. E., Harris, S. E., & Deary, I. J. (2019). Brain age and other bodily “ages”: Implications for neuropsychiatry. *Molecular Psychiatry*, 24, 266–281.
- de Lange, A.-M. G., Kaufmann, T., van der Meer, D., Maglanoc, L. A., Alnæs, D., Moberget, T., Douaud, G., Andreassen, O. A., & Westlye, L. T. (2019). Population-based neuroimaging reveals traces of childbirth in the maternal brain. *Proceedings of the National Academy of Sciences of the United States of America*, 116(44), 22341–22346.
- Di Biase, M. A., Tian, Y. E., Bethlehem, R. A. I., Seidlitz, J., Alexander-Bloch, A. F., Yeo, B. T. T., & Zalesky, A. (2023). Mapping human brain charts cross-sectionally and longitudinally. *Proceedings of the National Academy of Sciences of the United States of America*, 120, e2126798120.
- Feldt-Rasmussen, U., Hughes, D., Sunder-Plassmann, G., Shankar, S., Nedd, K., Olivetto, I., Ortiz, D., Ohashi, T., Hamazaki, T., Skuban, N., Yu, J., Barth, J. A., & Nicholls, K. (2020). Long-term efficacy and safety of migalastat treatment in Fabry disease: 30-month results from the open-label extension of the randomized, phase 3 ATTRACT study. *Molecular Genetics and Metabolism*, 131, 219–228.
- Gabusi, I., Pontillo, G., Petracca, M., Battocchio, M., Bosticardo, S., Costabile, T., Daducci, A., Pane, C., Riccio, E., Pisani, A., Brunetti, A., Schiavi, S., & Cocozza, S. (2022). Structural disconnection and functional reorganization in Fabry disease: A multimodal MRI study. *Brain Communications*, 4, fcac187.
- Germain, D. P. (2010). Fabry disease. *Orphanet Journal of Rare Diseases*, 5, 30.
- Germain, D. P., Altarescu, G., Barriales-Villa, R., Mignani, R., Pawlaczyk, K., Pieruzzi, F., Terry, W., Vujkovic, B., & Ortiz, A. (2022). An expert consensus on practical clinical recommendations and guidance for patients with classic Fabry disease. *Molecular Genetics and Metabolism*, 137, 49–61.
- Huang, G., Liu, Z., van der Maaten, L., & Weinberger, K. Q. (2017). Densely connected convolutional networks. *Proceedings of the IEEE Conference on Computer Vision and Pattern Recognition (CVPR)*, 2017, pp. 4700–4708. Retrieved from https://openaccess.thecvf.com/content_cvpr_2017/html/Huang_Densely_Connected_Convolutional_CVPR_2017_paper.html
- Kaufmann, T., van der Meer, D., Doan, N. T., Schwarz, E., Lund, M. J., Agartz, I., Alnæs, D., Barch, D. M., Baur-Streubel, R., Bertolino, A., Bettella, F., Beyer, M. K., Bøen, E., Borgwardt, S., Brandt, C. L., Buitelaar, J., Celius, E. G., Cervinka, S., Conzelmann, A., ... Westlye, L. T. (2019). Common brain disorders are associated with heritable patterns of apparent aging of the brain. *Nature Neuroscience*, 22, 1617–1623.
- Kolodny, E., Fellgiebel, A., Hilz, M. J., Sims, K., Caruso, P., Phan, T. G., Politei, J., Manara, R., & Burlina, A. (2015). Cerebrovascular involvement in Fabry disease: Current status of knowledge. *Stroke*, 46, 302–313.
- Lee, P.-L., Kuo, C.-Y., Wang, P.-N., Chen, L.-K., Lin, C.-P., Chou, K.-H., & Chung, C.-P. (2022). Regional rather than global brain age mediates cognitive function in cerebral small vessel disease. *Brain Communications*, 4, fcac233.
- Leonardsen, E. H., Peng, H., Kaufmann, T., Agartz, I., Andreassen, O. A., Celius, E. G., Espeseth, T., Harbo, H. F., Høgestøl, E. A., Lange, A.-M. d., Marquand, A. F., Vidal-Piñeiro, D., Roe, J. M., Selbæk, G., Sørensen, Ø., Smith, S. M., Westlye, L. T., Wolfers, T., & Wang, Y. (2022). Deep neural networks learn general and clinically relevant representations of the ageing brain. *Neuroimage*, 256, 119210.
- Mignani, R., Pieruzzi, F., Berri, F., Burlina, A., China, B., Gallieni, M., Pieroni, M., Salviati, A., & Spada, M. (2016). FABry STabilization indEX (FASTEX): An innovative tool for the assessment of clinical stabilization in Fabry disease. *Clinical Kidney Journal*, 9, 739–747.
- Nowak, A., Beuschlein, F., Sivasubramanian, V., Kasper, D., & Warnock, D. G. (2022). Lyso-Gb3 associates with adverse long-term outcome in patients with Fabry disease. *Journal of Medical Genetics*, 59, 287–293.
- Paavilainen, T., Lepomäki, V., Saunavaara, J., Borra, R., Nuutila, P., Kantola, I., & Parkkola, R. (2013). Diffusion tensor imaging and brain volumetry in Fabry disease patients. *Neuroradiology*, 55, 551–558.
- Paszke, A., Gross, S., Massa, F., Lerer, A., Bradbury, J., Chanan, G., Killeen, T., Lin, Z., Gimelshein, N., Antiga, L., Desmaison, A., Kopf, A., Yang, E., DeVito, Z., Raison, M., Tejani, A., Chilamkurthy, S., Steiner, B., Fang, L., ... Chintala, S. (2019). PyTorch: An imperative style, high-performance deep learning library. In *Advances in neural information processing systems* (Vol. 32). Curran Associates Retrieved from <https://proceedings.neurips.cc/paper/2019/hash/bdca288fee7f92f2bfa9f701272740-Abstract.html>
- Pontillo, G., Cocozza, S., Brunetti, A., Brescia Morra, V., Riccio, E., Russo, C., Saccà, F., Tedeschi, E., Pisani, A., & Quarantelli, M. (2018). Reduced intracranial volume in Fabry disease: Evidence of abnormal neurodevelopment? *Frontiers in Neurology*, 9, 672.
- Rombach, S. M., Smid, B. E., Linthorst, G. E., Dijkgraaf, M. G. W., & Hollak, C. E. M. (2014). Natural course of Fabry disease and the effectiveness of enzyme replacement therapy: A systematic review and meta-analysis: Effectiveness of ERT in different disease stages. *Journal of Inherited Metabolic Disease*, 37, 341–352.
- Rost, N. S., Cloonan, L., Kanakis, A. S., Fitzpatrick, K. M., Azzariti, D. R., Clarke, V., Lourenco, C. M., Germain, D. P., Politei, J. M., Homola, G. A., Sommer, C., Üçeyler, N., & Sims, K. B. (2016). Determinants of white matter hyperintensity burden in patients with Fabry disease. *Neurology*, 86, 1880–1886.
- Schiffmann, R., & Moore, D. F. (2006). Neurological manifestations of Fabry disease. In A. Mehta, M. Beck, & G. Sunder-Plassmann (Eds.), *Fabry disease: Perspectives from 5 years of FOS*. Oxford PharmaGenesis Retrieved from <http://www.ncbi.nlm.nih.gov/books/NBK11602/>
- Shi, Y., Mao, H., Gao, Q., Xi, G., Zeng, S., Ma, L., Zhang, X., Li, L., Wang, Z., Ji, W., He, P., You, Y., Chen, K., Shao, J., Mao, X., Fang, X., & Wang, F. (2022). Potential of brain age in identifying early cognitive impairment in subcortical small-vessel disease patients. *Frontiers in Aging Neuroscience*, 14, 973054.
- Springenberg, J. T., Dosovitskiy, A., Brox, T., & Riedmiller, M. (2015). Striving for simplicity: The all convolutional net. *arXiv*. Retrieved from <http://arxiv.org/abs/1412.6806>
- Steinbach, E. J., & Harshman, L. A. (2022). Impact of chronic kidney disease on brain structure and function. *Frontiers in Neurology*, 13, 797503. <https://doi.org/10.3389/fneur.2022.797503>

- Tanveer, M., Ganaie, M. A., Beheshti, I., Goel, T., Ahmad, N., Lai, K.-T., Huang, K., Zhang, Y.-D., Del Ser, J., & Lin, C.-T. (2023). Deep learning for brain age estimation: A systematic review. *Information Fusion*, 96, 130–143.
- Tian, Y. E., Cropley, V., Maier, A. B., Lautenschlager, N. T., Breakspear, M., & Zalesky, A. (2022). Biological aging of human body and brain systems. medRxiv. <https://doi.org/10.1101/2022.09.03.22279337v1>
- Tustison, N. J., Avants, B. B., Cook, P. A., Zheng, Y., Egan, A., Yushkevich, P. A., & Gee, J. C. (2010). N4ITK: Improved N3 bias correction. *IEEE Transactions on Medical Imaging*, 29, 1310–1320.
- Ullivi, L., Kanber, B., Prados, F., Davagnanam, I., Merwick, A., Chan, E., Williams, F., Hughes, D., Murphy, E., Lachmann, R. H., Wheeler-Kingshott, C. A. M. G., Cipolotti, L., & Werring, D. J. (2020). White matter integrity correlates with cognition and disease severity in Fabry disease. *Brain*, 143, 3331–3342.
- Vardarli, I., Rischpler, C., Herrmann, K., & Weidemann, F. (2020). Diagnosis and screening of patients with Fabry disease. *Ther Clin Risk Manag*, 16, 551–558.
- Vidal-Pineiro, D., Wang, Y., Krogsrud, S. K., Amlie, I. K., Baaré, W. F. C., Bartres-Faz, D., Bertram, L., Brandmaier, A. M., Drevon, C. A., Düzel, S., Ebmeier, K., Henson, R. N., Junqué, C., Kievit, R. A., Kühn, S., Leonardsen, E., Lindenberg, U., Madsen, K. S., Magnussen, F., ... Fjell, A. (2021). Individual variations in “brain age” relate to early-life factors more than to longitudinal brain change. *Elife*, 10, e69995.
- Wagen, A. Z., Coath, W., Keshavan, A., James, S.-N., Parker, T. D., Lane, C. A., Buchanan, S. M., Keuss, S. E., Storey, M., Lu, K., Macdougall, A., Murray-Smith, H., Freiburger, T., Cash, D. M., Malone, I. B., Barnes, J., Sudre, C. H., Wong, A., Pavisic, I. M., ... Schott, J. M. (2022). Life course, genetic, and neuropathological associations with brain age in the 1946 British Birth Cohort: A population-based study. *Lancet Healthy Longevity*, 3, e607–e616.
- Winkler, A. M., Ridgway, G. R., Webster, M. A., Smith, S. M., & Nichols, T. E. (2014). Permutation inference for the general linear model. *NeuroImage*, 92, 381–397.
- Wood, D. A., Kafiabadi, S., Busaidi, A. A., Guilhem, E., Montvila, A., Lynch, J., Townend, M., Agarwal, S., Mazumder, A., Barker, G. J., Ourselin, S., Cole, J. H., & Booth, T. C. (2022). Accurate brain-age models for routine clinical MRI examinations. *NeuroImage*, 249, 118871.

SUPPORTING INFORMATION

Additional supporting information can be found online in the Supporting Information section at the end of this article.

How to cite this article: Montella, A., Tranfa, M., Scaravilli, A., Barkhof, F., Brunetti, A., Cole, J., Gravina, M., Marrone, S., Riccio, D., Riccio, E., Sansone, C., Spinelli, L., Petracca, M., Pisani, A., Coccozza, S., & Pontillo, G. (2024). Assessing brain involvement in Fabry disease with deep learning and the brain-age paradigm. *Human Brain Mapping*, 45(5), e26599. <https://doi.org/10.1002/hbm.26599>